

Disentangling Pauli Blocking of Atomic Decay from Cooperative Radiation and Atomic Motion in a 2D Fermi Gas

Thomas Bilitewski^{1,2}, Asier Piñeiro Orioli^{1,2}, Christian Sanner¹, Lindsay Sonderhouse¹, Ross B. Hutson¹,
Lingfeng Yan¹, William R. Milner¹, Jun Ye¹, and Ana Maria Rey^{1,2}

¹JILA, National Institute of Standards and Technology and Department of Physics, University of Colorado,
Boulder, Colorado 80309, USA

²Center for Theory of Quantum Matter, University of Colorado, Boulder, Colorado 80309, USA



(Received 10 August 2021; accepted 17 February 2022; published 4 March 2022)

The observation of Pauli blocking of atomic spontaneous decay via direct measurements of the atomic population requires the use of long-lived atomic gases where quantum statistics, atom recoil, and cooperative radiative processes are all relevant. We develop a theoretical framework capable of simultaneously accounting for all these effects in the many-body quantum degenerate regime. We apply it to atoms in a single 2D pancake or arrays of pancakes featuring an effective Λ level structure (one excited and two degenerate ground states). We identify a parameter window in which a factor of 2 extension in the atomic lifetime clearly attributable to Pauli blocking should be experimentally observable in deeply degenerate gases with $\sim 10^3$ atoms. We experimentally observe a suppressed excited-state decay rate, fully consistent with the theory prediction of an enhanced excited-state lifetime, on the $^1S_0 - ^3P_1$ transition in ^{87}Sr atoms.

DOI: [10.1103/PhysRevLett.128.093001](https://doi.org/10.1103/PhysRevLett.128.093001)

Introduction.—Spontaneous emission emerges from the interaction of an excited atom with the vacuum of electromagnetic field modes [1,2]. It depends on the atomic internal structure but also on the density of states of the joint atom-photon system, which can be engineered by shaping the environment as widely demonstrated in cavity [3–7], circuit [8–13], and waveguide QED [14–16].

The emission rate can also be modified by Fermi statistics and Pauli blocking of the motional states into which an excited atom can decay. Since this effect was first pointed out [17], there have been a variety of subsequent theoretical explorations [18–26]. However, the experimental observation of Pauli blocking of radiation has been difficult due to the complex interplay of cooperative effects and atomic motion. Cooperative effects, arising from the virtual exchange of photons between atoms and the resulting dipolar interactions, can also enhance or suppress the radiative decay rate of the system [27–39], especially at the high densities required for Pauli blocking. At the same time, the emission process couples the internal dynamics to the motional states, leading to competition between the recoil kick during emission and the extent of the Fermi sea that blocks the decay.

Recent experiments have for the first time observed Pauli blocking through measurements of light scattered by atomic ensembles [40–42]. There, the mentioned undesirable competing effects were minimized by performing angular-resolved measurements to select low momentum transfer processes and by using a far detuned probe to

minimize cooperative dipolar processes and suppress the number of excited atoms.

However, an observation of enhanced lifetimes due to Pauli blocking by direct measurements of the excited-state population has yet to be demonstrated. Resonantly exciting a significant fraction of atoms to the excited state to subsequently measure their decay may result in significant dipolar interaction effects in striking contrast to scattering experiments. Moreover, working on a slow transition enabling time-resolved observation of the excited-state population poses the challenge that radiative decay rates and cooperative effects become comparable with the Fermi energy and associated motional degrees of freedom, which all need to be taken into account.

In this Letter, we develop a theoretical framework based on a master equation formulated in momentum space capable of describing the full dipolar dynamics of optically excited atoms confined in two dimensions (see Fig. 1) or in stacks of two-dimensional pancakes. While the few-body two-level problem can be treated exactly [26], our framework goes beyond this limit and, instead, is developed to tackle multilevel atomic ensembles in the interacting quantum degenerate regime. There, prior approaches fail since they account for Pauli blocking in a semiclassical noninteracting setting [23–25], include interactions for atoms at frozen positions, neglecting the recoil momentum [27–39], treat two-level systems in static motional states [43,44], neglecting motional dynamics, and do not account for the multilevel structure required for the Pauli blocking mechanism described here.

Our key finding is that a highly imbalanced ultracold Fermi gas excited by a resonant π pulse (which suppresses coherences) can feature at $T/T_F \sim 0.1$ (with T_F the Fermi temperature) up to 50% Pauli suppression at peak densities of 10^{14} cm^{-3} in a parameter regime where cooperative effects only affect the lifetime weakly. We perform measurements on the $^1S_0 - ^3P_1$ transition in fermionic ^{87}Sr at $T/T_F = 0.6$ with a natural lifetime of $\Gamma^{-1} = 21.3 \mu\text{s}$. Working with this long-lived narrow transition enables our experiment to spectroscopically resolve the multilevel structure and implement time-resolved measurements of the excited-state population dynamics. We observe an up to 20% reduction of the decay rate of the excited-state population, thus providing both theoretical predictions and direct experimental evidence for an enhanced lifetime of an optically excited state due to Pauli blocking.

Model.—We analyze first the case of a Fermi gas in a single pancake in the regime where only the ground-state harmonic oscillator mode $n_{0,z}$ is occupied, but motion is allowed in x and y [Fig. 1(a)]. For simplicity, we work with two-dimensional plane waves in x, y as our single-particle atomic basis, labeled by the momentum $\mathbf{k} = (k_x, k_y)$.

We consider an effective Λ -type internal level structure [Fig. 1(b)] with two internal ground states as the minimal system, allowing strong Pauli blocking even under full excitation of one of the states, but note that our results can be straightforwardly extended to more general multilevel

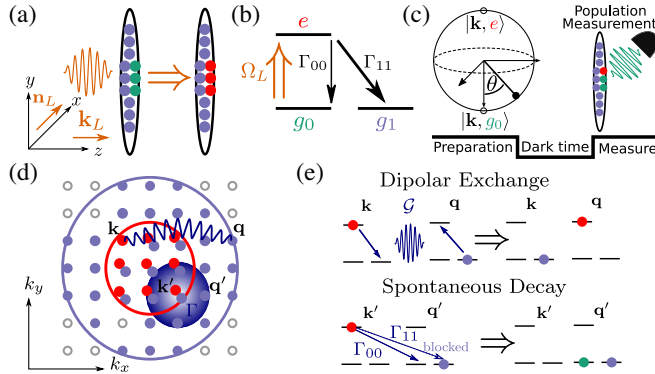


FIG. 1. (a) A 2D cloud of atoms is optically excited by a laser pulse with Rabi frequency Ω_L and wave vector \mathbf{k}_L propagating perpendicularly to the 2D plane and linearly polarized (\mathbf{n}_L) along x . (b) Internal level structure (Λ system), with one excited state e and two ground states g_α . The single-particle decay rate for $e \rightarrow g_\alpha$ is $\Gamma_{\alpha\alpha}$. (c) Protocol: after state preparation, atoms evolve freely and decay during a dark time t , followed by population measurement. (d) In plane momentum space (k_x, k_y) with two Fermi seas (red and blue circles). Filled circles denote occupied states. Interaction processes involving virtual exchange of photons between atoms at \mathbf{k} and \mathbf{q} are depicted as a wiggly line; single-particle spontaneous decay proportional to Γ are illustrated as the circular region (blue shading) around \mathbf{k}' . (e) Processes included in the master equation. Top: dipolar exchange between atoms in momenta \mathbf{k} and \mathbf{q} . Bottom: spontaneous decay from \mathbf{k}' to \mathbf{q}' .

systems. For specificity we focus on the $^1S_0(F = 9/2)$ to $^3P_1(F = 11/2)$ transition of ^{87}Sr , with the $m_F = -9/2$ excited state as e and the $m_F = -9/2, -7/2$ ground states as g_0 and g_1 , respectively, and set the quantization axis along x . We assume the presence of a magnetic field large enough to suppress transitions to other levels (which are omitted in the figure). The atoms are initially in an incoherent mixture with N_0 atoms in g_0 and N_1 in g_1 . This configuration features π and σ^- polarized decay, at rates $\Gamma_{00} = 2/11\Gamma$ and $\Gamma_{11} = 9/11\Gamma$, respectively, with $\Gamma^{-1} = 21.3 \mu\text{s}$ [45].

Atoms are excited by a short laser pulse with pulse area θ and then let to evolve and decay for some time t in the dark, after which the total excited-state population is measured [Fig. 1(c)]. We focus on the effective decay rate $\gamma_{\text{eff}}(\theta) = \lim_{t \rightarrow 0} \dot{N}_{ee}(t)/N_{ee}(0)$ obtained at initial time for the total number of excitations $N_{ee}(t)$. While the decay rate can change with time, in the cases discussed here, the decay at early times is well approximated by an exponential decay with rate γ_{eff} .

The initial excitation laser with wave number \mathbf{k}_L is propagating along the strongly confined z direction and linearly polarized (\mathbf{n}_L) along x so that it only excites g_0 atoms to e [Fig. 1(b)]. Because of the strong confinement along z , the motional state does not change during excitation: the Rabi pulse transfers a g_0 atom with momentum \mathbf{k} into the superposition $\cos(\theta/2)|g_0, \mathbf{k}, n_{0,z}\rangle + \sin(\theta/2)|e, \mathbf{k}, n_{0,z}\rangle$ [Fig. 1(c)], where $\theta = \Omega_L t$ with the Rabi coupling Ω_L of the $g_0 - e$ transition. The pulse is assumed to be fast, so we can ignore any interactions during it.

To describe the dynamics during the dark time, we start from the usual atom-light Hamiltonian and perform a Born-Markov approximation leading to a multilevel master equation (ME) with dipolar interactions [46]. We further only keep resonantly coupled pairs of modes \mathbf{k} and \mathbf{q} and neglect momentum changing collisions (see Supplemental Material [47]), which is justified at early times by the lack of coherences in the initial state between different momentum modes. For the atomic density matrix, this leads [47] to the following ME, $\dot{\hat{\rho}} = -i[\hat{H}, \hat{\rho}] + \mathcal{L}(\hat{\rho})$ with

$$\hat{H} = \sum_{\alpha, \beta} \left(\sum_{\mathbf{k}, \mathbf{q}} \Delta_{\alpha\beta}^{\mathbf{k}\mathbf{k}, \mathbf{q}\mathbf{q}} \hat{c}_{e, \mathbf{k}}^\dagger \hat{c}_{g_\beta, \mathbf{q}}^\dagger \hat{c}_{g_\alpha, \mathbf{k}} \hat{c}_{e, \mathbf{q}} + \sum_{\mathbf{k} \neq \mathbf{q}} \Delta_{\alpha\beta}^{\mathbf{k}\mathbf{q}, \mathbf{q}\mathbf{k}} \hat{c}_{e, \mathbf{k}}^\dagger \hat{c}_{g_\beta, \mathbf{q}}^\dagger \hat{c}_{g_\alpha, \mathbf{q}} \hat{c}_{e, \mathbf{k}} \right), \quad (1)$$

$$\mathcal{L}(\hat{\rho}) = \sum_{\alpha, \beta} \left(\sum_{\mathbf{k}, \mathbf{q}} \Gamma_{\alpha\beta}^{\mathbf{k}\mathbf{k}, \mathbf{q}\mathbf{q}} (2\hat{\sigma}_{g_\beta e}^{\mathbf{q}\mathbf{q}} \hat{\rho} \hat{\sigma}_{e g_\alpha}^{\mathbf{k}\mathbf{k}} - \{\hat{\sigma}_{e g_\alpha}^{\mathbf{k}\mathbf{k}} \hat{\sigma}_{g_\beta e}^{\mathbf{q}\mathbf{q}}, \hat{\rho}\}) + \sum_{\mathbf{k} \neq \mathbf{q}} \Gamma_{\alpha\beta}^{\mathbf{k}\mathbf{q}, \mathbf{q}\mathbf{k}} (2\hat{\sigma}_{g_\beta e}^{\mathbf{q}\mathbf{k}} \hat{\rho} \hat{\sigma}_{e g_\alpha}^{\mathbf{k}\mathbf{q}} - \{\hat{\sigma}_{e g_\alpha}^{\mathbf{k}\mathbf{q}} \hat{\sigma}_{g_\beta e}^{\mathbf{q}\mathbf{k}}, \hat{\rho}\}) \right). \quad (2)$$

Here, $\hat{\sigma}_{e,g_\alpha}^{\mathbf{k}\mathbf{q}} = \hat{c}_{e\mathbf{k}}^\dagger \hat{c}_{g_\alpha,\mathbf{q}}$, and $\hat{c}_{e,\mathbf{k}}^\dagger$ ($\hat{c}_{g_\alpha,\mathbf{k}}^\dagger$) creates a fermion in the e (g_α) state with in plane momentum $\mathbf{k} = (k_x, k_y)$ in the harmonic oscillator ground state $n_{0,z}$ along z .

The terms $\Delta_{\alpha\beta}^{\mathbf{k}\mathbf{l},\mathbf{m}\mathbf{n}}$ ($\Gamma_{\alpha\beta}^{\mathbf{k}\mathbf{l},\mathbf{m}\mathbf{n}}$) describe coherent (incoherent) exchange of photons of the relevant transitions $\alpha, \beta = 0, 1$ between two atoms in the corresponding internal and motional states [Figs. 1(d) and 1(e)]. They are defined as projections of the real (Re) and imaginary part (Im) of Green's tensor G as $\Delta_{\alpha\beta}^{\mathbf{i}\mathbf{j},\mathbf{k}\mathbf{l}} = \mathbf{d}_\alpha^T G_{\text{Re}}^{\mathbf{i}\mathbf{j},\mathbf{k}\mathbf{l}} \bar{\mathbf{d}}_\beta$, $\Gamma_{\alpha\beta}^{\mathbf{i}\mathbf{j},\mathbf{k}\mathbf{l}} = \mathbf{d}_\alpha^T G_{\text{Im}}^{\mathbf{i}\mathbf{j},\mathbf{k}\mathbf{l}} \bar{\mathbf{d}}_\beta$, where $\mathbf{d}_\alpha = C_\alpha \mathbf{n}_\alpha$, given in terms of the Clebsch-Gordan coefficient C_α and the polarization vector \mathbf{n}_α [$\mathbf{n}_0 = \mathbf{e}_x$, $\mathbf{n}_1 = (\mathbf{e}_y + i\mathbf{e}_z)/\sqrt{2}$], and \mathbf{d}^T and $\bar{\mathbf{d}}$ denote the transpose and complex conjugate, respectively. Green's tensor is $G(r) = (3\Gamma/4)\{[\mathbf{I} - \hat{\mathbf{r}} \otimes \hat{\mathbf{r}}](e^{ik_0 r}/k_0 r) + [\mathbf{I} - 3\hat{\mathbf{r}} \otimes \hat{\mathbf{r}}][ie^{ik_0 r}/(k_0 r)^2] - [e^{ik_0 r}/(k_0 r)^3]\}$, with the wave vector k_0 of the ground-excited-state transition. The matrix elements $G^{\mathbf{i}\mathbf{j},\mathbf{k}\mathbf{l}}$ are defined as $G^{\mathbf{i}\mathbf{j},\mathbf{k}\mathbf{l}} = \int d\mathbf{r} d\mathbf{r}' \bar{\phi}_i(\mathbf{r}) \phi_j(\mathbf{r}) G(\mathbf{r}-\mathbf{r}') \bar{\phi}_k(\mathbf{r}') \phi_l(\mathbf{r}')$, where $\phi_{\mathbf{k}}(x,y,z) = (1/\sqrt{A})e^{i(k_x x + k_y y)}\psi_0(z)$. The area A is chosen to approximate a harmonically trapped gas with trapping frequency $\omega_\perp = 2\pi \times 150$ Hz [47].

We emphasize that, in contrast to models considering multilevel atoms with static motional states, e.g., for atoms deeply confined in optical lattices [46], the second line of the Lindblad operator [Eq. (2)] contains momentum changing terms, which are crucial to correctly capture Pauli blocking in bulk Fermi gases.

We then derive equations of motion by using a mean-field approximation, which factorizes four-operator terms as products of two-operator terms (see Supplemental Material [47]). Given the uncorrelated initial conditions, this treatment is well justified at short times. We further assume that the dynamics is dominated by the momentum diagonal elements of the density matrix $\rho_{\mathbf{q}\mathbf{q}}^{\mu\nu} = \langle \hat{c}_{\mu,\mathbf{q}}^\dagger \hat{c}_{\nu,\mathbf{q}} \rangle$, where $\mu, \nu = e, g_0, g_1$, given the lack of momentum off-diagonal coherences in the initial state. Under these approximations the population of the excited state in momentum \mathbf{q} evolves as

$$\begin{aligned} \frac{d\rho_{\mathbf{q}\mathbf{q}}^{ee}}{dt} = & \sum_\alpha \sum_{\mathbf{k}} -2\Gamma_{\alpha\alpha}^{\mathbf{k}\mathbf{q},\mathbf{q}\mathbf{k}} (1 - \rho_{\mathbf{k}\mathbf{k}}^{g_\alpha g_\alpha}) \rho_{\mathbf{q}\mathbf{q}}^{ee} \\ & + \sum_{\alpha,\beta} \sum_{\mathbf{k}} i(\mathcal{G}_{\alpha\beta}^{\mathbf{q}\mathbf{q},\mathbf{k}\mathbf{k}} \rho_{\mathbf{q}\mathbf{q}}^{e g_\alpha} \rho_{\mathbf{k}\mathbf{k}}^{g_\beta e} - \bar{\mathcal{G}}_{\alpha\beta}^{\mathbf{q}\mathbf{q},\mathbf{k}\mathbf{k}} \rho_{\mathbf{q}\mathbf{q}}^{g_\beta e} \rho_{\mathbf{k}\mathbf{k}}^{e g_\alpha}), \end{aligned} \quad (3)$$

where $\mathcal{G}_{\alpha\beta}^{\mathbf{k}\mathbf{k},\mathbf{q}\mathbf{q}} = \Delta_{\alpha\beta}^{\mathbf{k}\mathbf{k},\mathbf{q}\mathbf{q}} + i\Gamma_{\alpha\beta}^{\mathbf{k}\mathbf{k},\mathbf{q}\mathbf{q}}$. The first line corresponds to the spontaneous decay process $|e, \mathbf{q}, n_{0,z}\rangle \rightarrow |g_\alpha, \mathbf{k}, n_{0,z}\rangle$ at a rate set by $\Gamma_{\alpha\alpha}^{\mathbf{q}\mathbf{k},\mathbf{k}\mathbf{q}}$, which accounts for the momentum conservation in the emission process, and is Pauli suppressed by the factor $1 - \rho_{\mathbf{k}\mathbf{k}}^{g_\alpha g_\alpha}$. Thus, the ME in momentum space naturally recovers Pauli blocking for arbitrary multilevel structures and generic geometries, while also including the most relevant cooperative effects,

such as superradiance and subradiance, that emerge from the terms in the second line. The latter depend on the coherences $\rho^{e g_\alpha}$ between the excited and the ground-state atoms and have contributions from the coherent (Δ) and incoherent dipolar exchange processes (Γ).

Pauli blocking in noninteracting atoms.—We start by studying the first line of Eq. (3) fully neglecting interaction effects and note the close resemblance to prior semiclassical approaches [24], where the decay of the atoms is dictated solely by the volume of the available phase space. To gain intuition note that $\Gamma_{\alpha\alpha}^{\mathbf{q}\mathbf{k},\mathbf{k}\mathbf{q}}$ mediates the decay of an atom e with momentum \mathbf{q} to the ground state g_α at momentum \mathbf{k} if $|\mathbf{k} - \mathbf{q}| \leq k_0$ (2D) or $|\mathbf{k} - \mathbf{q}| = k_0$ (3D) [47]. This decay will be Pauli blocked if the corresponding state is occupied due to the factor $1 - \rho_{\mathbf{k}\mathbf{k}}^{g_\alpha g_\alpha}$. Consequently, in the presence of a Fermi sea of ground-state atoms, the decay rate will be reduced. The degree of Pauli blocking will depend on the ratio of k_0 to k_F (controlled by the density) and the mean occupation within the Fermi sea (set by the temperature of the gas).

To illustrate this phenomenology, we show in Fig. 2 the rate $\gamma_{\text{eff}}^{\text{nonint}}/\Gamma$ for an initially balanced Fermi gas with $N_0 = N_1$ noninteracting atoms and full excitation of all g_0 atoms to the e state (i.e., $\theta = \pi$), as a function of the temperature T/T_F . In this case the maximal Pauli suppression achievable is $\Gamma_{11}/\Gamma \sim 81\%$ when all decay channels into g_1 are blocked. We compare the 3D (dashed) to the strongly confined 2D system (solid) for a range of N (colors), i.e., of k_0/k_F . Most notably, we observe a strong enhancement of Pauli blocking in 2D compared to 3D, over a significantly larger range of temperatures.

This can be understood as follows. First, the axial confinement changes the energy spectrum and thus the

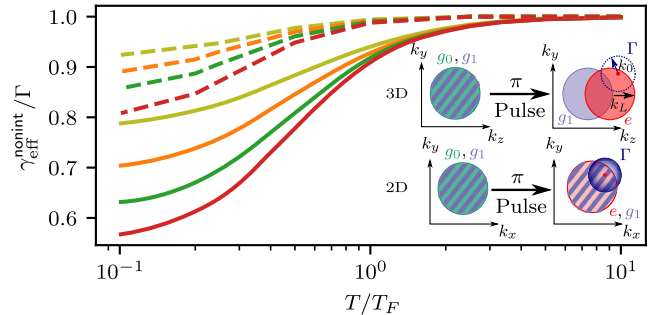


FIG. 2. Pauli blocking of spontaneous emission for noninteracting atoms. Decay rate $\gamma_{\text{eff}}^{\text{nonint}}/\Gamma$ vs T/T_F comparing 3D (dashed) to 2D (solid) for $N_0 = N_1$ and $\theta = \pi$. $N_{2D} = 100, 200, 400, 800$ for the colored lines (top to bottom), corresponding to $k_0/k_F = 1.51, 1.26, 1.07, 0.90$. N_{3D} is chosen such that $k_0/k_F^{3D} = k_0/k_F^{2D}$ at these atom numbers. Inset: illustration of the initial state before and after laser excitation in 2D and 3D. Colored circles denote Fermi seas of different atomic levels and striped areas denote an overlap of two Fermi seas. Blue circles of radius k_0 labeled Γ show the states reachable by a spontaneous decay process.

density of states. This results in a higher mean occupation fraction in 2D and, consequently, stronger Pauli blocking than in 3D for the same k_0/k_F . Second, the initial laser excitation imparts a momentum kick to the atoms in 3D that displaces the excited population away from the unexcited ground-state Fermi sea, facilitating decay to unoccupied states (inset of Fig. 2). In contrast, in 2D for laser excitation along the strongly confined direction, the motional states are unaffected, enhancing the probability to decay to an already occupied state.

Interplay of dipolar interactions with Pauli blocking.— In Fig. 3 we study how $\gamma_{\text{eff}}^{\text{nonint}}$ (dashed lines) is modified by dipolar induced cooperative effects using the full ME (solid lines) as a function of the pulse area θ for a balanced gas, $N_0 = N_1$. At $\theta = \pi$, interactions have no effect on γ_{eff} due to the absence of initial coherences. However, for smaller θ and increasing N , there is an intricate competition between interactions and Pauli blocking. Note the modifications from θ affect exclusively the $e \rightarrow g_0$ transition. On the one hand, lowering θ results in a higher population in the g_0 ground state $\sim \cos^2(\theta/2)$, which increases Pauli blocking of the $e \rightarrow g_0$ decay channel for noninteracting atoms. On the other hand, interaction effects become stronger at low θ , leading to an enhanced normalized superradiant decay that scales as $\sim \cos^2(\theta/2)$ [47]. Importantly, the superradiant enhancement also scales with N . This interplay leads to dominant Pauli blocking and thus lower decay rates at low atom numbers and dominant cooperatively enhanced emission and faster radiative decay at high densities as θ decreases.

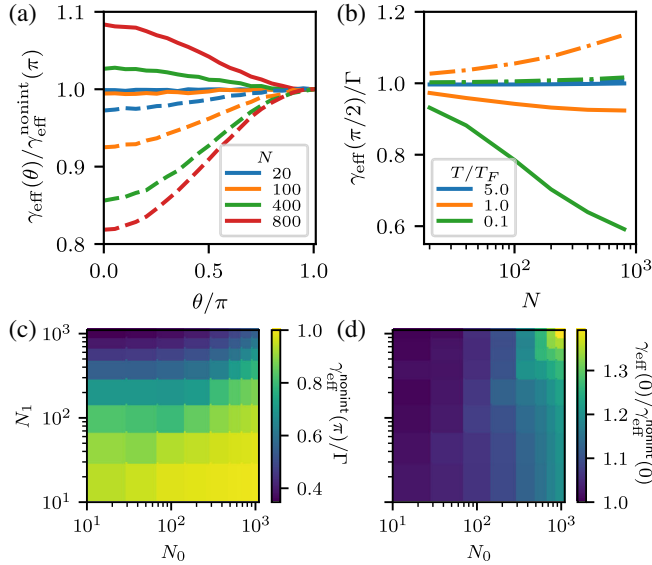


FIG. 3. Interplay of dipolar interactions and Pauli blocking in 2D. (a) $\gamma_{\text{eff}}(\theta)/\gamma_{\text{eff}}^{\text{nonint}}(\pi)$ comparing the full ME (solid) to the noninteracting part (dashed) at $T/T_F = 0.1$ for different $N = N_0 = N_1$. (b) Decay rate $\gamma_{\text{eff}}/\Gamma$ at $\theta = \pi/2$ vs N at different temperatures comparing the full ME (solid) to the frozen atom approximation (dash-dotted lines). (c) Decay rate $\gamma_{\text{eff}}^{\text{nonint}}(\pi)$ vs N_0 and N_1 . (d) Interaction effects quantified by $\gamma_{\text{eff}}/\gamma_{\text{eff}}^{\text{nonint}}$ for $\theta \rightarrow 0$ vs N_0, N_1 . (c),(d) In thermal equilibrium for $T_0 = T_1$ and $T/T_{F,1} = 0.1$.

To demonstrate the importance of including atomic motion and its interplay with quantum statistics, we also compare the ME in momentum space to the usual frozen atom approximation (FA) [27–38], which is derived for atoms assumed to be at fixed positions in real space. We show the resulting γ_{eff} for a $\theta = \pi/2$ excitation as a function of the atom number N and temperature T/T_F in Fig. 3(b). The FA properly captures the superradiantly enhanced decay rate due to dipolar interactions. However, its inability to account for Pauli blocking results in incorrect predictions in the quantum degenerate regime and an incorrect scaling of the decay rate with N .

Finally, Figs. 3(c) and 3(d) explore the role of the imbalance N_1/N_0 of the initial populations of the two ground states on the effective decay rate. For noninteracting atoms it is highly advantageous to only excite a small fraction of atoms [24] to maximize Pauli blocking. This is demonstrated in Fig. 3(c), which shows the decay rate $\gamma_{\text{eff}}^{\text{nonint}}/\Gamma$ at $T/T_F = 0.1$ for $\theta = \pi$, predicting the largest suppression in the $N_1 \gg N_0$ regime. Interestingly, for the 2D system, even in the presence of superradiance as $\theta \rightarrow 0$, it is possible to minimize interaction effects while maintaining significant Pauli suppression ($\sim 66\%$) by choosing $N_1 \gg N_0$ as shown in Fig. 3(d). This is because only the N_0 atoms feature coherences and experience dipolar interactions at early times.

Comparison with experiment.—We compare our predictions to experimental measurements done on the $^1S_0 - ^3P_1$ transition in fermionic ^{87}Sr . The 7.5 KHz natural linewidth of this transition allows us to spectroscopically resolve the multilevel structure and to track the excited-state population dynamics in a time-resolved fashion. We consider an array of two-dimensional pancakes (inset of Fig. 4), realized by confining the initially 3D Fermi gas in a deep optical lattice along z . The extension of the theory and

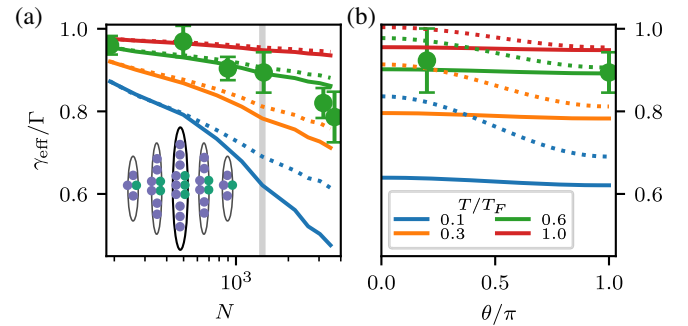


FIG. 4. Decay rates in stacked pancakes geometry. (a) Scaling of the decay rate γ_{eff} with N comparing the balanced case (dotted), $N_0 = N_1 = N$, to the highly imbalanced case (solid), $N_0 = 200, N_1 = N$, for a $\theta = \pi$ pulse. The gray shading denotes the fixed $N = 1500$ used in (b) $\gamma_{\text{eff}}/\Gamma$ vs θ . Temperatures indicated in the legend in (b), in the imbalanced case $T_0 = T_1$ and given with respect to $T_{F,1}$. Points with error bars are experimental data taken under the same conditions as the solid green lines.

details on the experimental preparation and measurement protocol are provided in the Supplemental Material [47].

Figure 4 shows experimental data available for the highly imbalanced scenario, demonstrating agreement with our predictions within errors (green points and lines). Figure 4(a) shows the effective decay rate $\gamma_{\text{eff}}/\Gamma$ as a function of the atom number, pulse area, and temperature, comparing a balanced (dotted) to the imbalanced case (solid) for a π pulse excitation. For $N \sim 4 \times 10^3$ and $T/T_F = 0.1$ corresponding to peak densities of 10^{14} cm^{-3} , we predict up to a factor of 2 enhancement in the atomic lifetime. In Fig. 4(b) we demonstrate the strong interaction effects present for balanced gases when preparing initial coherences due to superradiance. In contrast, we emphasize the weak dependence on θ in the imbalanced case, which demonstrates the lack of significant cooperative effects.

Outlook.—We theoretically predict enhanced lifetimes attributable to Pauli blocking. This prediction is supported by experimental observation of excited-state populations in imbalanced multilevel 2D Fermi gases. The good agreement of our theory treatment, which neglects many-body correlations, and the experimental observations support the validity of our treatment in the investigated regime and motivates further experimental work. Important future directions include the preparation of a deeply degenerate Fermi gas in 2D, where the differences between balanced and imbalanced cases become rather striking, as well as the exploration of conditions where the interplay of quantum statistics and correlations could modify more dramatically the radiative decay dynamics.

AFOSR Grant No. FA9550-18-1-0319 and its MURI Initiative, by the DARPA and ARO Grant No. W911NF-16-1-0576, the ARO single investigator Grant No. W911NF-19-1-0210, the NSF PHY1820885, NSF JILA-PFC PHY-1734006 Grants, NSF QLCI-2016244 Grant, DOE-QSA, and by NIST. C.S. thanks the Humboldt Foundation for support. The authors thank Nathan Schine and Joseph Thywissen for providing feedback on the Letter.

-
- [1] M. Born and P. Jordan, Zur quantenmechanik, *Z. Phys.* **34**, 858 (1925).
- [2] P. A. M. Dirac and N. H. D. Bohr, The quantum theory of the emission and absorption of radiation, *Proc. R. Soc. A* **114**, 243 (1927).
- [3] P. Berman, *Cavity Quantum Electrodynamics* (Academic Press, Boston, 1994).
- [4] J. M. Raimond, M. Brune, and S. Haroche, Manipulating quantum entanglement with atoms and photons in a cavity, *Rev. Mod. Phys.* **73**, 565 (2001).
- [5] H. J. Kimble, Strong interactions of single atoms and photons in cavity QED, *Phys. Scr.* **T76**, 127 (1998).
- [6] S. Haroche and D. Kleppner, Cavity quantum electrodynamics, *Phys. Today* **42**, 24 (1989).
- [7] S. Haroche, Cavity quantum electrodynamics: A review of Rydberg atom-microwave experiments on entanglement and decoherence, *AIP Conf. Proc.* **464**, 4566 (1999).
- [8] S. Haroche, M. Brune, and J. M. Raimond, From cavity to circuit quantum electrodynamics, *Nat. Phys.* **16**, 243 (2020).
- [9] A. Blais, A. L. Grimsmo, S. M. Girvin, and A. Wallraff, Circuit quantum electrodynamics, *Rev. Mod. Phys.* **93**, 025005 (2021).
- [10] G. Burkard, M. J. Gullans, X. Mi, and J. R. Petta, Superconductor-semiconductor hybrid-circuit quantum electrodynamics, *Nat. Rev. Phys.* **2**, 129 (2020).
- [11] A. Blais, R.-S. Huang, A. Wallraff, S. M. Girvin, and R. J. Schoelkopf, Cavity quantum electrodynamics for superconducting electrical circuits: An architecture for quantum computation, *Phys. Rev. A* **69**, 062320 (2004).
- [12] X. Gu, A. F. Kockum, A. Miranowicz, Y. xi Liu, and F. Nori, Microwave photonics with superconducting quantum circuits, *Phys. Rep.* **718–719**, 1102 (2017).
- [13] A. A. Clerk, K. W. Lehnert, P. Bertet, J. R. Petta, and Y. Nakamura, Hybrid quantum systems with circuit quantum electrodynamics, *Nat. Phys.* **16**, 257 (2020).
- [14] B. Kannan, M. J. Ruckriegel, D. L. Campbell, A. F. Kockum, J. Braumüller, D. K. Kim, M. Kjaergaard, P. Krantz, A. Melville, B. M. Niedzielski, A. Vepsäläinen, R. Winik, J. L. Yoder, F. Nori, T. P. Orlando, S. Gustavsson, and W. D. Oliver, Waveguide quantum electrodynamics with superconducting artificial giant atoms, *Nature (London)* **583**, 775 (2020).
- [15] D. Roy, C. M. Wilson, and O. Firstenberg, Colloquium: Strongly interacting photons in one-dimensional continuum, *Rev. Mod. Phys.* **89**, 021001 (2017).
- [16] A. S. Sheremet, M. I. Petrov, I. V. Iorsh, A. V. Poshakinskiy, and A. N. Poddubny, Waveguide quantum electrodynamics: Collective radiance and photon-photon correlations, *arXiv*: 2103.06824.
- [17] K. Helmerson, M. Xiao, and D. Pritchard, Radiative decay of densely confined atoms, in *International Quantum Electronics Conference* (Optical Society of America, Washington, DC, 1990).
- [18] J. Javanainen and J. Ruostekoski, Off-resonance light scattering from low-temperature Bose and Fermi gases, *Phys. Rev. A* **52**, 3033 (1995).
- [19] B. DeMarco and D. S. Jin, Exploring a quantum degenerate gas of fermionic atoms, *Phys. Rev. A* **58**, R4267 (1998).
- [20] J. Ruostekoski and J. Javanainen, Optical Linewidth of a Low Density Fermi-Dirac Gas, *Phys. Rev. Lett.* **82**, 4741 (1999).
- [21] B. DeMarco and D. S. Jin, Exploring a quantum degenerate gas of fermionic atoms, *Phys. Rev. A* **58**, R4267 (1998).
- [22] A. Görlitz, A. P. Chikkatur, and W. Ketterle, Enhancement and suppression of spontaneous emission and light scattering by quantum degeneracy, *Phys. Rev. A* **63**, 041601(R) (2001).
- [23] T. Busch, J. R. Anglin, J. I. Cirac, and P. Zoller, Inhibition of spontaneous emission in Fermi gases, *Europhys. Lett.* **44**, 16 (1998).
- [24] B. Shuve and J. H. Thywissen, Enhanced Pauli blocking of light scattering in a trapped Fermi gas, *J. Phys. B* **43**, 015301 (2010).

- [25] B. O’Sullivan and T. Busch, Spontaneous emission in ultracold spin-polarized anisotropic Fermi seas, *Phys. Rev. A* **79**, 033602 (2009).
- [26] R. M. Sandner, M. Müller, A. J. Daley, and P. Zoller, Spatial Pauli blocking of spontaneous emission in optical lattices, *Phys. Rev. A* **84**, 043825 (2011).
- [27] B. Zhu, J. Cooper, J. Ye, and A. M. Rey, Light scattering from dense cold atomic media, *Phys. Rev. A* **94**, 023612 (2016).
- [28] R. H. Lehberg, Radiation from an n -atom system. I. General formalism, *Phys. Rev. A* **2**, 883 (1970).
- [29] D. F. V. James, Frequency shifts in spontaneous emission from two interacting atoms, *Phys. Rev. A* **47**, 1336 (1993).
- [30] J. Ruostekoski and J. Javanainen, Quantum field theory of cooperative atom response: Low light intensity, *Phys. Rev. A* **55**, 513 (1997).
- [31] A. A. Svidzinsky, J.-T. Chang, and M. O. Scully, Cooperative spontaneous emission of n atoms: Many-body eigenstates, the effect of virtual lamb shift processes, and analogy with radiation of n classical oscillators, *Phys. Rev. A* **81**, 053821 (2010).
- [32] T. Bienaim, M. Petruzzo, D. Bigerni, N. Piovella, and R. Kaiser, Atom and photon measurement in cooperative scattering by cold atoms, *J. Mod. Opt.* **58**, 1942 (2011).
- [33] T. Bienaimé, N. Piovella, and R. Kaiser, Controlled Dicke Subradiance from a Large Cloud of Two-Level Systems, *Phys. Rev. Lett.* **108**, 123602 (2012).
- [34] W. Guerin, M. O. Araújo, and R. Kaiser, Subradiance in a Large Cloud of Cold Atoms, *Phys. Rev. Lett.* **116**, 083601 (2016).
- [35] R. T. Sutherland and F. Robicheaux, Coherent forward broadening in cold atom clouds, *Phys. Rev. A* **93**, 023407 (2016).
- [36] S. L. Bromley, B. Zhu, M. Bishof, X. Zhang, T. Bothwell, J. Schachenmayer, T. L. Nicholson, R. Kaiser, S. F. Yelin, M. D. Lukin, A. M. Rey, and J. Ye, Collective atomic scattering and motional effects in a dense coherent medium, *Nat. Commun.* **7**, 11039 (2016).
- [37] S. J. Roof, K. J. Kemp, M. D. Havey, and I. M. Sokolov, Observation of Single-Photon Superradiance and the Cooperative Lamb Shift in an Extended Sample of Cold Atoms, *Phys. Rev. Lett.* **117**, 073003 (2016).
- [38] P. Weiss, M. O. Arajo, R. Kaiser, and W. Guerin, Subradiance and radiation trapping in cold atoms, *New J. Phys.* **20**, 063024 (2018).
- [39] W. Guerin, M. Rouabah, and R. Kaiser, Light interacting with atomic ensembles: Collective, cooperative and mesoscopic effects, *J. Mod. Opt.* **64**, 895 (2017).
- [40] C. Sanner, L. Sonderhouse, R. B. Hutson, L. Yan, W. R. Milner, and J. Ye, Pauli blocking of atom-light scattering, *Science* **374**, 979 (2021).
- [41] Y. Margalit, Y.-K. Lu, F. Ç. Top, and W. Ketterle, Pauli blocking of light scattering in degenerate fermions, *Science* **374**, 976 (2021).
- [42] A. B. Deb and N. Kjærgaard, Observation of Pauli blocking in light scattering from quantum degenerate fermions, *Science* **374**, 972 (2021).
- [43] F. Damanet, D. Braun, and J. Martin, Master equation for collective spontaneous emission with quantized atomic motion, *Phys. Rev. A* **93**, 022124 (2016).
- [44] F. Damanet, D. Braun, and J. Martin, Cooperative spontaneous emission from indistinguishable atoms in arbitrary motional quantum states, *Phys. Rev. A* **94**, 033838 (2016).
- [45] T. Nicholson, S. Campbell, R. Hutson, G. Marti, B. Bloom, R. McNally, W. Zhang, M. Barrett, M. Safronova, G. Strouse, W. Tew, and J. Ye, Systematic evaluation of an atomic clock at 2×10^{-18} total uncertainty, *Nat. Commun.* **6**, 6896 (2015).
- [46] A. Piñeiro Orioli and A. M. Rey, Subradiance of multilevel fermionic atoms in arrays with filling $n \geq 2$, *Phys. Rev. A* **101**, 043816 (2020).
- [47] See Supplemental Material at <http://link.aps.org/supplemental/10.1103/PhysRevLett.128.093001>, which also includes Refs. [48–54], for additional details on the derivation of the master equation and the mean-field equations of motion, including the explicit expressions for Green’s functions and the extension of the theory to the array of pancakes, and the experimental sequence and measurement protocol.
- [48] T. Bilitewski, L. De Marco, J.-R. Li, K. Matsuda, W. G. Tobias, G. Valtolina, J. Ye, and A. M. Rey, Dynamical Generation of Spin Squeezing in Ultracold Dipolar Molecules, *Phys. Rev. Lett.* **126**, 113401 (2021).
- [49] L. Sonderhouse, C. Sanner, R. Hutson, A. Goban, T. Bilitewski, L. Yan, W. Milner, A. Rey, and J. Ye, Thermodynamics of a deeply degenerate $SU(n)$ -symmetric Fermi gas, *Nat. Phys.* **16**, 1216 (2020).
- [50] A. Rey, A. Gorshkov, C. Kraus, M. Martin, M. Bishof, M. Swallows, X. Zhang, C. Benko, J. Ye, N. Lemke, and A. Ludlow, Probing many-body interactions in an optical lattice clock, *Ann. Phys. (Amsterdam)* **340**, 311 (2014).
- [51] A. P. Koller, M. L. Wall, J. Munding, and A. M. Rey, Dynamics of Interacting Fermions in Spin-Dependent Potentials, *Phys. Rev. Lett.* **117**, 195302 (2016).
- [52] P. He, M. A. Perlin, S. R. Muleady, R. J. Lewis-Swan, R. B. Hutson, J. Ye, and A. M. Rey, Engineering spin squeezing in a 3D optical lattice with interacting spin-orbit-coupled fermions, *Phys. Rev. Research* **1**, 033075 (2019).
- [53] S. Smale, P. He, B. A. Olsen, K. G. Jackson, H. Sharum, S. Trotzky, J. Marino, A. M. Rey, and J. H. Thywissen, Observation of a transition between dynamical phases in a quantum degenerate Fermi gas, *Sci. Adv.* **5**, eaax1568 (2019).
- [54] M. A. Perlin, D. Barberena, M. Mamaev, B. Sundar, R. J. Lewis-Swan, and A. M. Rey, Engineering infinite-range $SU(n)$ interactions with spin-orbit-coupled fermions in an optical lattice, *Phys. Rev. A* **105**, 023326 (2022).